SCIENTIFIC REPORTS

OPEN

SUBJECT AREAS:
NANOWIRES
MATERIALS SCIENCE
NANOSCALE MATERIALS
MAGNETIC PROPERTIES AND MATERIALS

Received
8 March 2013

Accepted
13 September 2013

Published
29 October 2013

Correspondence and requests for materials should be addressed to A.B.K. (angelaklautau@gmail.com)

Complex magnetic structure of clusters and chains of Ni and Fe on Pt(111)

Manoel M. Bezerra-Neto[1], Marcelo S. Ribeiro[1], Biplab Sanyal[2], Anders Bergman[2], Roberto B. Muniz[3], Olle Eriksson[2] & Angela B. Klautau[1]

[1]Faculdade de Física, Universidade Federal do Pará, Belém, PA, Brazil, [2]Department of Physics and Astronomy, Uppsala University, 75120 Box 516 Sweden, [3]Instituto de Física, Universidade Federal Fluminense, 24210-340, Niterói, RJ, Brazil.

We present an approach to control the magnetic structure of adatoms adsorbed on a substrate having a high magnetic susceptibility. Using finite Ni-Pt and Fe-Pt nanowires and nanostructures on Pt(111) surfaces, our *ab initio* results show that it is possible to tune the exchange interaction and magnetic configuration of magnetic adatoms (Fe or Ni) by introducing different numbers of Pt atoms to link them, or by including edge effects. The exchange interaction between Ni (or Fe) adatoms on Pt(111) can be considerably increased by introducing Pt chains to link them. The magnetic ordering can be regulated allowing for ferromagnetic or antiferromagnetic configurations. Noncollinear magnetic alignments can also be stabilized by changing the number of Pt-mediated atoms. An Fe-Pt triangularly-shaped nanostructure adsorbed on Pt(111) shows the most complex magnetic structure of the systems considered here: a spin-spiral type of magnetic order that changes its propagation direction at the triangle vertices.

Magnetism of nanostructures adsorbed on metallic surfaces is a subject of intense research. One of the magnetic properties of nanostructures, which play an important role in the design of new devices, is the exchange interaction between their constituent atoms[1]. Depending on the strength and sign of the exchange interactions, one can achieve ferromagnetic or antiferromagnetic alignment, and even more complex spin structures in these nanostructures[2–5]. Recent experiments have shown how the exchange interaction between supported magnetic dimers can be determined[6–9]. Moreover, by using spin-resolved scanning tunneling microscopy, it is now possible to determine and control the spin direction of single atoms on metallic surfaces[2].

Concerning the magnetic behavior of one-dimensional atomic chains, an enhanced anisotropy and large magnetic moments have been reported for nanowires of Co on a Pt surface[10,11]. For very small coverages of Ni on a Pt surface, experimental studies have dealt with the peculiar structure and composition of these systems, indicating the formation of a one-dimensional ordered Ni-Pt alloy at the step edges of the Pt surface[12]. Several open questions involving the relationship between chemical and magnetic order in such nanostructures remain. Correlations between magnetism and atomic structure have also been experimentally investigated in Fe-Pt monolayer alloys[13] and corrugated Fe islands[13,14] on Pt surfaces, suggesting the formation of a complex magnetic phase, due to the influence of the local environment.

In this article, we present first-principles calculations of the electronic structure and magnetic properties of Ni and Fe adatoms, wires and nanostructures supported on a Pt (111) surface. This study has been motivated by an interesting discussion on the role of the mediating Pt atoms on the stable magnetic configurations of these nanostructures[12–14]. Here, the goal is the possibility of controlling and tailoring complex magnetic configurations on the atomic scale, by exploring the presence of magnetic frustrations. Furthermore, the use of indirect exchange coupling to perform logical operations between individual atomic spins is a challenge for nanospintronic research[1,15,16]. We investigate the Fe-Fe and Ni-Ni exchange interactions by increasing the interatomic distance of Fe and Ni dimers on Pt(111). We also discuss the dependence of these exchange couplings between the Fe and Ni atoms, when including Pt atoms, which are known to have high magnetic susceptibility. Interestingly, our results show that it is possible to tune the exchange interaction between magnetic adatoms (Fe or Ni) by varying the number of Pt atoms linking them. For instance, the exchange interaction between Ni (or Fe) adatoms can be considerably enhanced by introducing Pt chains to couple them. Moreover, the exchange interaction between the Ni (or Fe) atoms switches sign as the width of the Pt spacer thickness varies. Also, we show that not only a ferromagnetic or an antiferromagnetic configuration of magnetic adatoms can be adjusted by introducing non-magnetic chains to link them[17], but also a non-collinear magnetic ordering can be stabilized via the variation of the Pt-linker atoms, or by including edge effects in the choice of the system geometry.

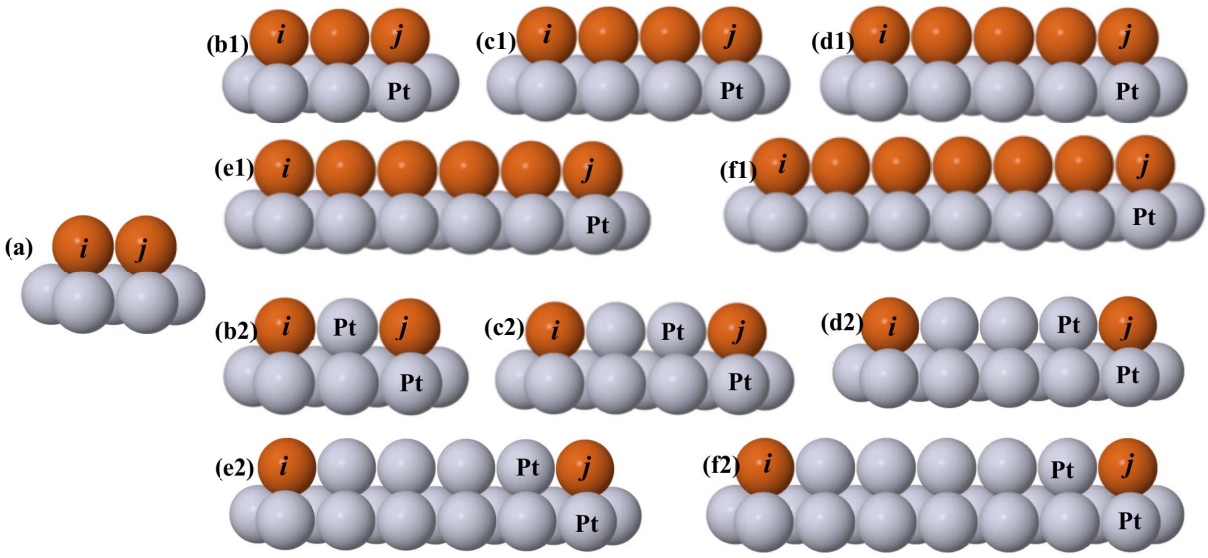

Figure 1 | Structures of the systems considered: (a) Dimer, ((b1)–(f1)) finite monoatomic chains of Ni or Fe, and alloyed ((b2)–(f2)) Fe (or Ni)-Pt chains adsorbed on a Pt(111) surface. The red (dark) and gray (light) balls indicate Fe (or Ni) and Pt atoms, respectively.

Results

Geometrical aspects. In order to study the complex correlation between structure and magnetism in one-dimensional chains on metallic surfaces, we performed calculations (*cf.* Methods section) for several Ni structures supported on Pt(111), of different size and geometry, as shown in Fig. 1 and 2. We have in our investigation considered the following systems: Ni adatom; Ni dimer (Fig. 1(a)); monoatomic Ni wires (Fig. 1(b1)–Fig. 1(f1)), and alloyed Ni-Pt chains (Fig. 1(b2)–Fig. 1(f2), Fig. 2(d)), with up to 7 atoms; triangular Ni trimer (Fig. 2(a)); double Ni wires (Fig. 2(b), Fig. 2(c)); step-edge alloyed Ni-Pt wires (Fig. 2(e)) and monoatomic Ni wires (Fig. 2(f)) with up to 5 atoms. These choices of structures for the alloyed Ni-Pt wires on Pt(111) are based on theoretical[18] and experimental[12] investigations, where in the latter, the formation of a one-dimensional ordered Ni/Pt alloy at the step edges of a Pt(997) surface was observed[12]. For some of the geometries in Figs. 1 and 2 we also considered Fe clusters and chains, see below.

Ni based linear chains. The magnetic moments for the Ni atoms are found to be rather sensitive to the number of nearest neighbor Ni and Pt atoms, and in general fewer neighbors yield higher magnetic moment (as shown in Fig. 3). Moreover, the presence of Ni-Pt mixing tends to decrease the local moment of the Ni atoms. This tendency is seen in Fig. 3, where we plot the average spin and orbital (with and without orbital polarization - OP[19]) moments as a function of the corresponding average number of nearest neighbors (Ni + Pt). The data in Fig. 3(a1) and Fig. 3(a2) give a linear decay of the spin moment with increasing number of nearest neighbor atoms (Fe, Ni or Pt). This can be understood from a tight binding analysis in which the band width is proportional to the square root of the coordination number. From such an analysis one can deduce that the maximum moment (M_{max}) possible, as a function of band filling, is proportional to the inverse of the square root of the coordination number, i.e. $m_{max} = C/\sqrt{(N)}$, where C is a constant. Making a Taylor expansion of this relation around some selected coordination, e.g. $N = 5$, results in an expression $M_{max} = M_{max}(N = 5) - C \cdot \Delta N$. This is roughly the behavior found in Fig. 3.

Regarding the values of the orbital moment values, a comparison between theory and experiment often indicates that OP overestimates the enhancement of the orbital moment by roughly a factor of 2. Therefore, it has been suggested[10] that better theoretical evaluations for the orbital moments can be obtained by dividing the Racah constant in the OP calculation by a factor of 2 or by taking an average between results obtained with and without the OP terms[20,21]. Our, results from such an average predict an high orbital moment for the Ni adatom on Pt(111) (~0.9 μ_B), and an orbital moment of around 0.3 μ_B/atom and 0.4 μ_B/atom should be observed in the limit of very large Ni nanowires on Pt(111), with and without a step, respectively. Note that an orbital moment of 0.30 μ_B/atom represents a large enhancement compared with the Ni bulk orbital moment (0.05 μ_B/

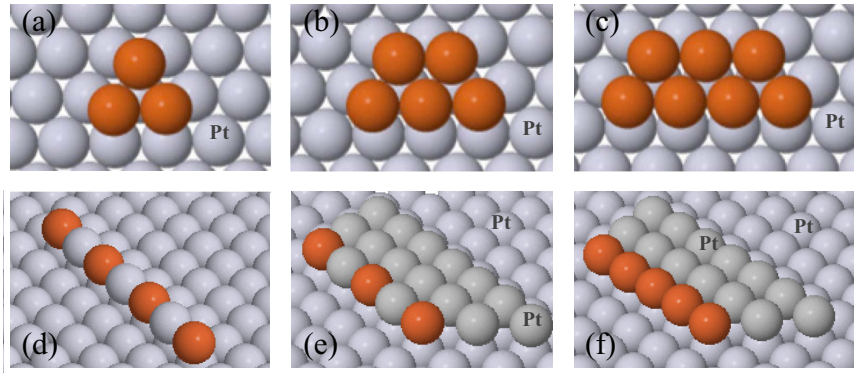

Figure 2 | Structures of the systems considered: (a) Triangular trimer, and (b)–(c) double-chains. (d) Alloyed and (e) step-edged alloyed Ni-Pt chains, and (f) monoatomic Ni wire at the step-edged on Pt(111) surface. The red (dark) and gray (light) balls indicate Ni (or Fe) and Pt atoms, respectively.

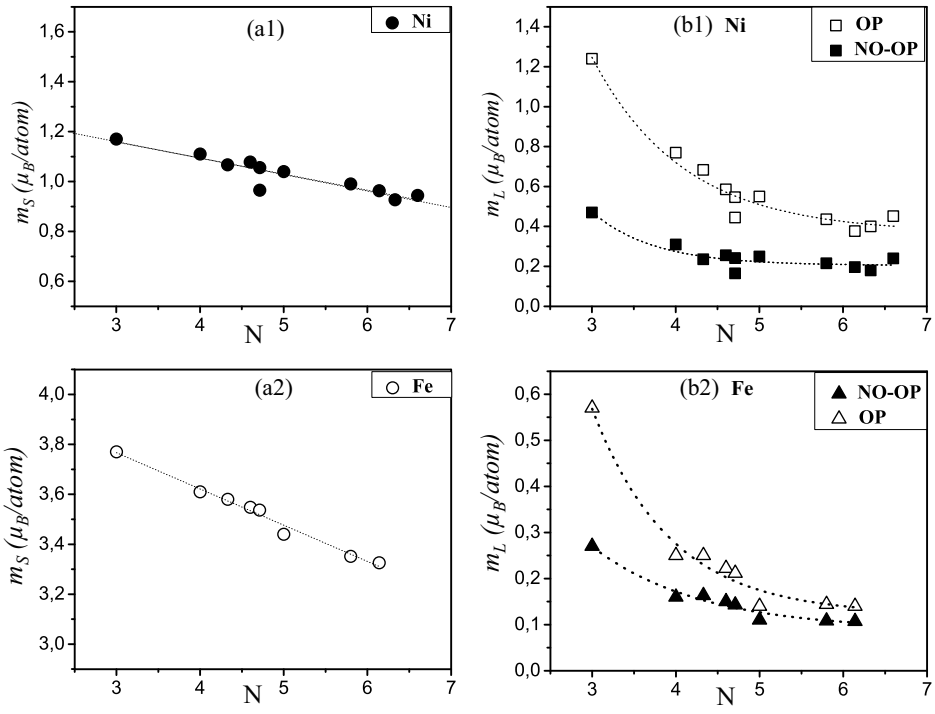

(c) N: Average number of (3*d and 4d*) first neighbors (Fe or Ni), (Pt)

N	3	4	4.33	4.5	4.6	4.67	4.71

N	4.71	5	5.8	6.14	6.33	6.6

Figure 3 | (a1) [a2] Average spin, m_S, and (b1) [b2] orbital moments, m_L, at Ni [Fe] sites on Pt(111), as a function of the average number of nearest neighbors (including substrate atoms) of Ni [Fe] and Pt (marked as N). OP (NO-OP) denotes calculations performed with (without) Orbital Polarization. (c) The values of N for geometries shown in Fig. 1 and Fig. 2. Note that in Fig. 3(c) the atoms of the substrate are not shown, only the atoms of the supported cluster. Grey spheres denote Fe or Ni atoms, open spheres denote Pt atoms.

atom)[22]. We find that the orbital and spin magnetic moments are coupled in parallel, which is also observed in bulk Fe and Ni, due to that the electronic shell is more than half filled. Spin induced moments on the Pt sites, which are nearest neighbors to Ni atoms, were also calculated, and they vary from 0.08 μ_B/atom to 0.30 μ_B/atom, where sites with larger number of Ni nearest neighbors present larger magnetic moments. The orbital contribution to the magnetic moment of Pt atoms is significant, with computed ratios of orbital moment (m_L) to spin moment (m_S) ranging from 0.3–0.6, for calculation without OP. When OP is included, the calculated m_L/m_S ratios vary between 0.5 and 0.8. For $Ni_m/Pt_n(111)$ multilayers, *ab initio* results[23] and XMCD measurements[24–26] also give large values for the induced moment of Pt at the Pt-Ni interface, and a similar behavior is found for the magnetic moments of Ni as a function of Pt neighbors. Nevertheless, to the best of our knowledge, there are no experimental results for the magnetic moments of Ni nanostructures on Pt(111).

In order to explore the origin of our calculated ground state magnetic configurations, we have computed the exchange-coupling parameters between Ni and Fe local moments for several nanowires deposited on Pt(111) substrate. Within the RS-LMTO-ASA method[32] the exchange integrals (J_{ij}) are calculated from perturbation theory in conjunction with multiple scattering theory of the electronic structure[33], assuming neighboring spins are rotated relative to each other by an infinitesimal amount from a collinear spin configuration. The convention we use is that the energy of the spin system is written in the form $-\sum'_{ij} J_{ij}\hat{e}_i\cdot\hat{e}_j$, where $\hat{e}_i$ is a unit vector along the direction of local magnetic moment at site i. Note that the magnitudes of the moments have been incorporated into the effective J_{ij} interactions. However, in the quantum Heisenberg model used to interpret the experiments reported in Ref. (7) one has $H = -\sum'_{ij}\tilde{J}_{ij}\mathbf{S}_i\cdot\mathbf{S}_j$. Therefore, in order to compare our calculated values of J_{ij} with the experimental ones $\tilde{J}_{ij}$, we may assume that $\mathbf{S} = S\hat{e}$, so $\tilde{J}_{ij} = J_{ij}/S^2$, where $S \approx m_s/2$.

The dependence of the exchange coupling parameters (J_{ij}) on the distance between the adatoms and the number and type of such atoms are shown in Fig. 4(a), for three different situations. (i) (squares) Ni dimers, with interatomic distances varying from 2.77Å to 8.31Å. (ii) (circles) Ni wires with different lengths, including 2–7 Ni atoms. Here J_{ij} values were calculated between the Ni atoms at the edges of the wires (denoted by sites i and j on Fig. 1(a),(b1)–(f1)). The third geometry considered is (iii) (triangles) Ni dimers, with different number of Pt atoms (from 1 to 5) separating the Ni atoms, in a geometry as is shown in Fig. 1(b2)–(f2). The interaction between nearest neighbor Ni atoms for different dimers is strong and

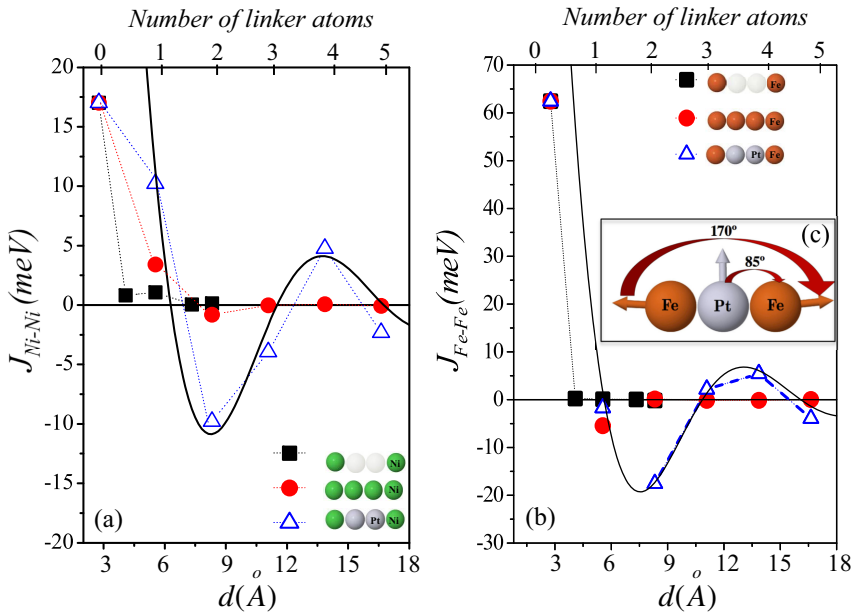

Figure 4 | (a) [b] Exchange coupling parameters (J_{Ni-Ni}) [J_{Fe-Fe}] between: (squares) Ni [Fe] dimers for different interatomic distances, (circles) Ni [Fe] atoms at the edge of monoatomic Ni [Fe] chains, and (triangles) Ni [Fe] atoms at the edges of Pt chains adsorbed on Pt(111) surface. The inset (c) shows the magnetic configuration and angles between magnetic moments for a Fe dimer separated by one Pt atom on a Pt(111) surface. Full lines refer to a RKKY model fitting (with an oscillation decaying as $1/d^2$ - see text) for the interaction between Fe (or Ni) adatoms mediated by Pt atoms on a Pt(111) surface.

ferromagnetic. The exchange interactions between Ni adatoms (situation (i), above), separated by 4.80Å and 5.54Å, remain ferromagnetic, but they are strongly reduced in magnitude. At further separations the exchange coupling decays to zero. For the Ni chains (situation (ii), described above), the J_{ij} values between Ni atoms at the edge of the chain are slightly enhanced in comparison to case (i), and for some distances the exchange interaction becomes antiferromagnetic between the edge atoms. However, taking into account all exchange interactions in these chains we find that for wires with length up to 1.1 nm the FM order prevails. The same behavior is obtained for the double and the step-edge Ni wires on Pt(111). Nevertheless, by introducing Pt chains between the Ni atoms (situation (iii), described above), the magnitude of the exchange interaction between Ni adatoms considerably increases, and the magnetic behavior is different. Ni atoms linked by one or two Pt atoms (Fig. 1(b2),(c2)) present exchange coupling interactions with the same magnitude, but with opposite signs. By introducing 3 or 5 Pt atoms linking Ni ad-atoms (Fig. 1(d2),(f2)), the Ni pair becomes antiferromagnetically coupled, whereas 4 Pt linker atoms (Fig. 1(e2)) lead to a ferromagnetic coupling between the Ni atoms. The value of the exchange coupling parameters (J_{Ni-Pt}) between a Ni atom and its Pt nearest neighbors located above the surface layer (in the surface layer) is always positive and of order of 1.4–2.7(0.7)*meV/atom*, which is weaker than the Ni-Ni interactions. For the ordered (step-edge) alloyed Ni-Pt chains, with only one Pt atom between Ni atoms (Fig. 2(d),(e)) we obtained a ferromagnetic configuration. Nevertheless, for alloyed Ni-Pt wires with 2 or 3 Pt linker atoms, we infer an antiferromagnetic configuration.

Fe based linear chains. We have also analyzed the magnetic properties of Fe nanostructures on Pt(111), as shown in Fig. 1 and Fig. 2(a)–(c). The values for the magnetic moments on Fe sites, shown in Fig. 3(a2,b2), follows the same behavior of the corresponding Ni nanostructures on Pt(111). Similarly, previous theoretical results reveal this dependence of the magnetic moments with the number of nearest neighbors for 3*d* atoms on a Pt(111) surface[10,27]. The strong hybridization between the Fe 3*d* and Pt 5*d* states induces large moments on Pt nearest neighbors localized above the surface with values that vary from 0.15 μ_B/atom to 0.37 μ_B/atom for the spin moments, and 0.10 μ_B/atom to 0.20 μ_B/atom for the orbital moments (without OP). It is worth noting that experimentally[13] an induced moment of ~0.27 μ_B/atom at the Pt site was suggested for Fe-Pt monolayer alloys on Pt surfaces. Concerning the spin (m_S) and orbital (m_L) moments of the Fe atoms, we find that in some systems they are not parallel to each other. For instance, for the triangular Fe trimer on Pt(111) (Fig. 2(a)), the angle between m_S and m_L on the Fe sites is approximately 10°. For the induced Pt magnetic moments, we obtained a parallel alignment between m_S and m_L.

In Fig. 4(b) we present the calculated J_{ij} between Fe atoms for dimers adsorbed on Pt(111), with the interatomic distance varying from 2.77Å to 8.31Å, and for Fe pairs linked by other Fe atoms or Pt chains, as shown in Fig. 1. We find that nearest neighbor Fe atoms in a dimer adsorbed on Pt(111) are strongly coupled ferromagnetically with $J_{Fe-Fe} = 61.2$ *meV* for a calculation without structural relaxations. An inward perpendicular relaxation towards the Pt(111) surface of 10% causes the exchange coupling parameter to decrease to $J_{Fe-Fe} = 39.4$ *meV*, without considerably changing the Fe local magnetic moments (they change by less than 0.1 μ_B/atom). As pointed out in the Methods section, in order to compare our theoretical results with the experimental value $\tilde{J}_{ij} = 16 \pm 1$ *meV* reported in Ref. (7), we note that the calculated values (J_{Fe-Fe}) should be divided by S^2, where $S \sim m_S/2$, leading to $J_{Fe-Fe}/S^2 = 18.9$ *meV* without relaxation, and 12.6 *meV* with 10% relaxation, which agree reasonably well with the observed value. For Fe pairs at further distances, and without atoms linking them, the magnitude of J_{Fe-Fe} decreases substantially. Adding another Fe atom to form a linear trimer (Fig. 1(b1)), the exchange interaction between Fe nearest neighbors decreases by ~30%, and a much weaker negative value is obtained for J_{Fe-Fe} between atoms at the edge of the chain. For larger Fe chains on Pt(111) (Fig. 1(c1–f1)), the exchange interaction between first neighbors remains strong and positive, and between Fe atoms at the edges oscillates, and is decaying to zero. For the Fe wires on Pt(111) the most stable magnetic configuration is the ferromagnetic one, when taking into account all interactions.

By including Pt chains to link Fe atoms on Pt(111) (Fig. 1(b2–f2)), a different scenario is revealed. In the case of one Pt atom inserted between Fe dimers (Fig. 1(b2)), the exchange coupling between the Fe atoms at the edge of the wire is negative and of the same order of magnitude as the positive exchange coupling between the Fe atom and the large induced moment at the Pt atom ($J_{Fe-Pt} = 5.4\ meV$). The competition between these interactions leads to the magnetic configuration shown in Fig. 4(c), where the Pt moment is almost perpendicular to the Fe moments, and a canted antiferromagnetic configuration is obtained for the Fe atoms. This canted magnetic configuration is also stabilized by the Dzyaloshinskii-Morya (DM) interaction, since it favors perpendicularly arranged moments. By inserting two Pt atoms linking Fe atoms (Fig. 1(c2)), this latter pair exhibits a strong antiferromagnetic coupling. The exchange interaction between an Fe atom with its nearest neighbor Pt localized above the surface is always ferromagnetic ($\sim 5\ meV$), and the value of J_{Pt-Pt} between first neighbors Pt atoms is much smaller ($\sim 0.1\ meV$). Hence, a collinear antiferromagnetic structure between the Fe atoms at the edges of the chain is obtained. The structures with three or four Pt atoms between Fe show ferromagnetic exchange interaction between the Fe pair, which is larger than the inter-atomic exchange interaction between Fe atoms at the edges of linear chains solely composed of Fe atoms. At larger distances of the Fe adatoms, and including five Pt in between, the exchange interaction between the Fe sites reverses its sign to become negative.

We also explored the interaction between Fe chains on Pt(111), carrying out calculations for Fe double-wires, where the inter-wire distance was increased from 2.77Å to 11.09Å (Fig. 5((a),(b1),(c1)), and also decorated laterally by Pt atoms (Fig. 5((b2),(c2),(d)). The exchange interaction between the Fe chains is shown in Fig. 5(e). Note that this interaction is calculated as the average interaction between all Fe atoms on one chain in Fig. 5, and all the Fe atoms of the other chain. Analogous to the behavior of the Fe adatoms (Fig. 4), the magnitude of the exchange interaction between Fe chains is enhanced by introducing Pt atoms to link the Fe chains.

We now proceed with an analysis of the exchange interactions displayed in Figs. 4 and 5. As shown in Fig. 4 (full lines), the interaction between Fe (or Ni) adatoms, mediated by Pt atoms, may be fitted by a Ruderman-Kittel-Kasuya-Yoshida (RKKY) model[28–30,50,51] ($J_{Fe-Fe}(d) \propto cos(2k_F d + \beta)/d^n$, $n = 2$), where d is the distance between the atoms, β is a phase, and the Fermi wavelength ($\lambda_F = 2\pi/k_F$) has been fixed to the value known from Pt(111) surface state ($\lambda_F \approx 1.6\ nm$)[31]. The interaction between line defects, as shown in Fig. 5(e) (full [red] line), could also be analyzed in terms of the RKKY interaction, while the oscillation decays as $1/d^{5/2}$ ($J/N \propto (cos(2k_F d) + sin(2k_F d))/d^{5/2}$)[29]. Both Fig. 4 and 5(e) shows that the RKKY expressions makes a rather good fit to the calculated data, which demonstrates that it is indeed the RKKY interaction which is relevant. This motivates a detailed comparison between the exchange interaction between two Fe (or Ni) atoms at the edge of a chain, when there is either Pt connecting the edge atoms, or if there are Fe (or Ni) atoms connecting the edge atoms. This comparison is shown in Fig. 4(a) for Fe and Fig. 4(b) for Ni. It is seen that magnetic edge atoms (Fe or Ni) connected by Pt atoms, have a much stronger long ranged exchange interaction, compared to magnetic edge atoms that are connected by other magnetic atoms of the same kind, i.e. Fe (or Ni). Hence it seems that the RKKY interaction is heavily damped when the medium mediating it has a large spin-polarization or is composed of the same element.

In order to analyze this phenomenon, it is useful to recapitulate that the coupling between local moments on sites i and j is given by[32,33]

$$J_{ij} = \frac{ImTr}{4\pi}\int_{-\infty}^{E_F}\left[\delta_i(E)G_{ij}^{\uparrow}(E)\delta_j(E)G_{ji}^{\downarrow}(E)\right]dE, \qquad (1)$$

where the trace is over orbital indices, and G_{ij}^{σ} is the propagator between sites i and j, for electrons with spin σ, in the ferromagnetic configuration. The quantity $\delta_i(E)$ has units of energy and yields the local exchange splitting between the up- and down-spin bands, at site i. Since in transition metals the exchange potential acting on d states is substantially larger than that acting on $s - p$ states, the spin splitting of s- and p-like states is relatively small. This might lead one to neglect the latter and restrict the trace over orbitals in the Eq. (1) to those with d-symmetry. Moreover, the values of $\delta_i(E)$ for wires composed by Fe (or Ni) atoms linked by Pt or linked by Fe (or Ni)

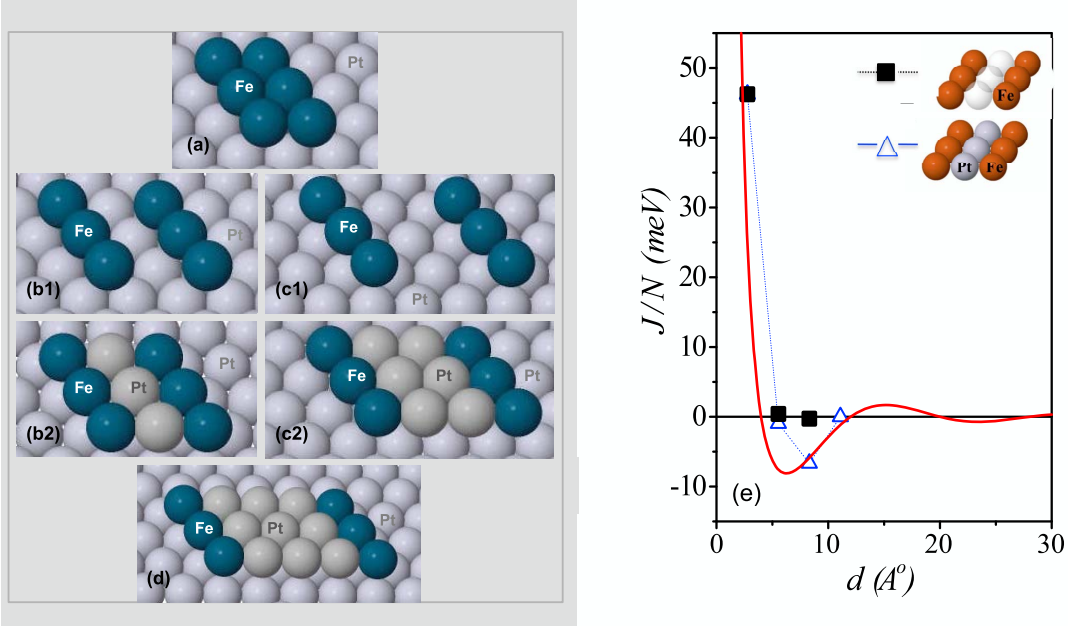

Figure 5 | (a)–(d) Schematic representation of double Fe chains on Pt(111); the blue (dark) and gray (light) balls indicate Fe and Pt atoms, respectively. (e) Exchange interaction (J/N) between two parallel Fe chains divided by the number of Fe atoms (N) in each chain; full squares (open triangles) refer to J/N between ad-chains without (with) Pt atoms linking the Fe chains on Pt(111). (Red) Full line representing the fitting of RKKY interaction between Fe line defects on Pt(111) surface.

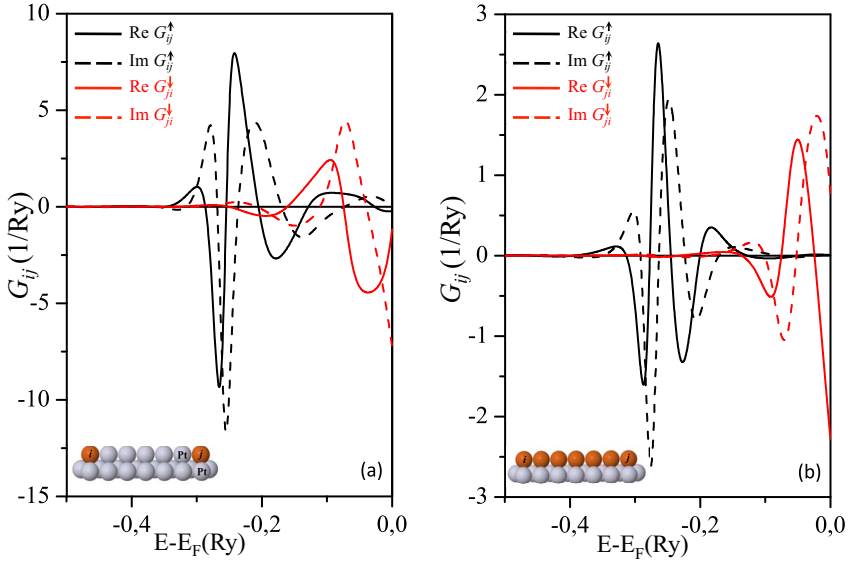

Figure 6 | The propagator between *d* states in Eq. (1): Real (full lines) and Imaginary (dashed lines) part of the Green's functions, G_{ij}^{σ}, for electrons with spin $\sigma = \uparrow$ (black lines), and $\sigma = \downarrow$ (red lines) for (a) an Fe pair linked by 5 Pt atoms on Pt(111), and (b) a monoatomic Fe chain with 7 atoms adsorbed on Pt(111). The inset shows the geometry of the calculation, where grey balls represent Pt atoms and orange balls represent Fe atoms.

atoms are similar, indicating that the large difference between the J_{ij} values in these two situations comes from the different behavior of the propagators, as discussed below. Evaluating Eq. (1), it can been shown that, in order to have non-zero J_{ij}, one needs products of $ReG_{ij}^{\uparrow} \cdot ImG_{ji}^{\downarrow}$, and (or) $ReG_{ji}^{\downarrow} \cdot ImG_{ij}^{\uparrow}$ to be non-zero. This indicates that a considerable overlap between $ReG_{ij}^{\uparrow}$ and $ImG_{ji}^{\downarrow}$ (or between $ReG_{ji}^{\downarrow}$ and $ImG_{ij}^{\uparrow}$) functions, is needed over a large energy interval, in order for J_{ij} values to be different from zero. Taking as an example the system composed by two Fe atoms separated by 5 Pt atoms (see Fig. 6(a)), we obtained indeed a large overlap between the G_{ij} propagators for electrons with different spin, resulting in an exchange coupling parameter of $J_{ij} \sim -4$ *meV*. For the monoatomic Fe wire with the same size (Fig. 6(b)), there is essentially no overlap between these functions, and $J_{ij} \sim 0$. An analogous behavior was also verified for the other nanowires studied here. The larger overlap obtained for the Fe atoms linked by Pt atoms, is a consequence of the more extended states involved, i.e. the Pt 5*d* orbitals, which allow a more long-ranged interaction.

Triangular clusters. In order to verify the combined influence of edge effects[34,35] and the intriguing exchange coupling between Fe atoms linked by Pt atoms on the magnetic properties of these nanomagnets, we also performed calculations for triangular Fe-Pt nanostrucutures on Pt(111), as shown in Fig. 7. It is important to note that calculations of pair exchange can for particular systems become quite complex, and higher order interactions or tensorial contributions have been discussed[36]. This is particularly true for relativistic theories, where the magnetic anisotropy starts to come close to the exchange interaction, e.g. in systems with large spin-orbit effects like Pt. The present calculation did include spin-orbit coupling, and the spin-configurations reported here contain on equal footing exchange and spin-orbit effects. However, for the calculation of pair-exchange we used the simpler non-relativistic formulation of Ref. 33.

For a triangle composed by 3 atoms of Fe in the vertices connected (attached) by Pt atoms (Fig. 7(a1)), we calculated a negative exchange interaction between the Fe atoms ($J_{Fe-Fe} = -12.2$ *meV*), and a positive value between Fe and Pt nearest neighbor atoms ($J_{Fe-Pt} = +4.1$ *meV*). This nature of exchange interactions, coupled with the geometric frustration imposed by the structure, leads to the noncollinear magnetic structure shown in Fig. 7(a1), where the Fe spin moments ($\sim 3.6\ \mu_B$) are not inplane and the angle between them is $\sim 120^{\circ}$. The orbital moments at the Fe sites ($m_L \sim 0.1\ \mu_B$) are not aligned to the spin moments, with angles between them of order of 30°. The induced moments on the Pt sites ($m_S = 0.3\ \mu_B$ and $m_L = 0.15\ \mu_B$) are almost parallel to the nearest neighbor Fe moments. To extract the influence of the Pt atoms linking the Fe atoms on the magnetic structure of this nanostructure, we also performed calculations for only the 3 atoms of Fe located in the vertices of a triangle on Pt(111), as shown in Fig. 7(a2). In this example the exchange interaction between the Fe atoms is negative, but much weaker ($J_{Fe-Fe} = -0.1$ *meV*). In this case the exchange interaction is small, and hence the effect of the DM interaction and the MAE become relatively more important. As a result of the competition between these three interactions, we obtained a canted ferromagnetic structure, shown in Fig. 7(a2), where the Fe spin moments ($\sim 3.7\ \mu_B$) are almost perpendicular to the plane and the angle between them is $\sim 20^{\circ}$. Fig. 7(a2) displays a magnetic structure that possesses a lower symmetry than the C_{3v} symmetry of the cluster geometry. When spin-orbit coupling is treated together with the exchange splitting of the valence states, in general the symmetry of the combined crystalline and magnetic structure is lower than that of the crystalline structure alone[37–39]. For example, for bcc Fe the crystalline structure is cubic but when the easy axis of the magnetization ([001] direction) is taken into account, the combined magnetic and crystalline structure has a reduced symmetry, tetragonal to be precise, which also leads to a small exchange-striction. Fig. 7(a2), as well as Fig. 7(b1) and (b2), display a similar effect. To be more concrete, the spin-structure in Fig. 7(a2) does not rotate into itself under a 120 degrees rotation along an axis out of the plane. This also implies that there are several possible magnetic configurations that are degenerate with the one shown in Fig. 7(a2), provided that the relative orientations of the spins are preserved. For instance, the spin structures obtained under a $\pm$ 120 degree rotation of Fig. 7(a2) are degenerate with the one in Fig. 7(a2).

In Fig. 7(b1,b2) we present our calculated results for ground state magnetic configuration of a Fe-Pt triangularly-shaped nanostructure adsorbed on Pt(111), where 15 Fe atoms form the lateral edges of a triangle, and its inside is decorated by 6 atoms of Pt. For this complex magnetic structure, the Fe spin moments form a spin-spiral type of magnetic order that changes its propagation direction at the triangle

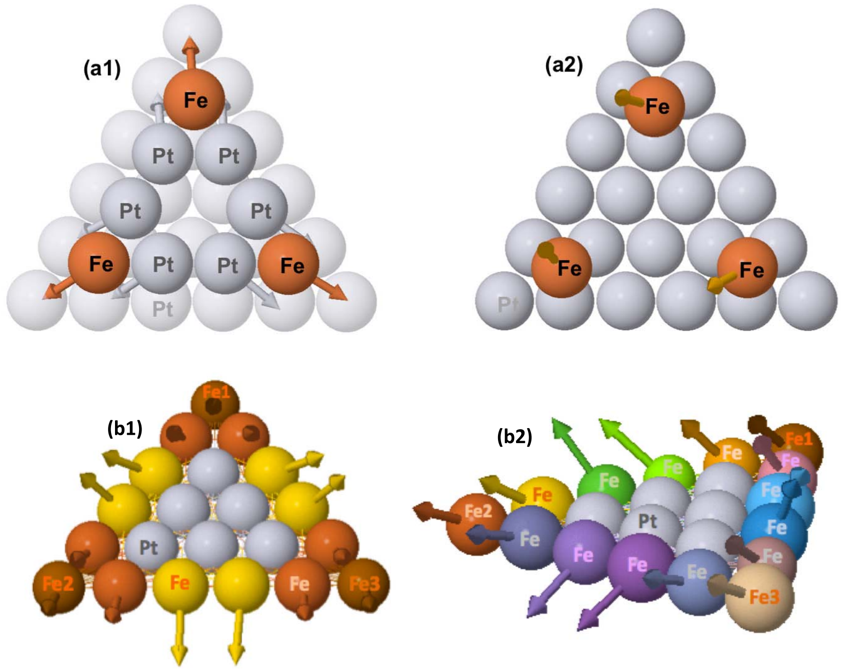

Figure 7 | Noncollinear magnetic configurations for Fe-Pt triangularly-shaped structures on Pt(111). (a1) a triangle composed by 3 atoms of Fe in the vertices connected by Pt atoms. (a2) three atoms of Fe in the vertices of a triangle. (b1) and (b2) top and lateral views, respectively, of a Fe-Pt nanostructure where 15 Fe atoms form the lateral edges of a triangle, and its inside is decorated by 6 atoms of Pt.

vertices. To evaluate the possible subtle dependence of this complex noncollinear magnetism to the Dzyaloshinski-Moriya (DM) interactions[27,40], we also performed calculations without spin-orbit coupling, obtaining a canted FM order as the most stable magnetic configuration. Therefore, as depicted in Fig. 7(b1,b2), calculations taking into account spin-orbit coupling show a spin twist, that is caused by non-negligible contributions of the DM interaction.

Discussion

We presented *ab initio* calculations of arrays of Fe and Ni adatoms adsorbed on a Pt(111) surface. We predict a huge orbital moment for a Ni adatom adsorbed on Pt(111) surface. The magnetic behavior of 1D monoatomic and alloyed Ni-Pt atomic chains is revealed. Monoatomic Ni chains display a ferromagnetic configuration with large magnetic moments per Ni atom. For the alloyed chains the magnetic behavior is different. Ni atoms linked by one or two Pt atoms present exchange coupling with the same magnitude, but with opposite signs, revealing the possibility of stabilizing ferromagnetic or antiferromagnetic configurations in alloyed Ni-Pt nanowires on a Pt(111) surface. For Fe-Pt nanomagnets on Pt(111), we have found large induced moments on the Pt atoms, leading to competing Fe-Pt and Fe-Fe pairwise exchange interactions, and a strong dependence of the exchange interactions between Fe atoms on the number of linker Pt atoms. As a consequence, either a ferromagnetic or an antiferromagnetic configuration between magnetic Fe adatoms can be stabilized depending on the Pt spacer thickness. Moreover, a non-collinear magnetic ordering can be obtained for non-frustrated geometries tuned by Pt-mediated atoms. These complex ordering phenomena are in general due to a competition between exchange interactions between different atoms and atom types, the Dzyaloshinskii-Morya interaction and the magnetic anisotropy energy.

We have also demonstrated that the interatomic exchange interaction has much longer range between two Fe (or Ni) atoms separated by a chain of Pt atoms, compared to a chain of Fe (or Ni) atoms, and provided a microscopic explanation for this unexpected finding. Also, for a triangular shaped Fe-Pt nanostructure on Pt(111), the edge effect was explored, showing a complex magnetic structure such as a spin-spiral type of magnetic order with a pattern which changes its propagation direction at the triangle edges. Some of the magnetic structures identified here have a low symmetry enabling a complex energy landscape. The types of low symmetry magnetic structures investigated here, have recently been discussed in terms of unusual magnetization dynamics in which the relationship between switching time and driving forces can be seen as an analog of non-Newtonian dynamics[41]. In the work of Etz *et al.*[41] the switching imposed by an external magnetic field was found to have a non-monotonous dependence upon field strength. Further studies of this effect on the nanostructures presented here will be undertaken in near future.

Methods

The calculations were performed using the first-principles, self-consistent RS-LMTO-ASA (real space - linear muffintin orbital - atomic sphere approximation) method[42,43], which has been generalized to the treatment of non-collinear magnetism[4,44,45]. This method is based on the LMTO-ASA formalism[46], and uses the recursion method[47] to solve the eigenvalue problem directly in real space. The calculations presented here are fully self-consistent and performed within the local spin density approximation (LSDA)[48]. We included the spin-orbit coupling term $\alpha L.S$ self-consistently at each variational step, where α is the spin-orbit coupling strength, L and S are the orbital and spin angular momentum operators[19,20]. We also present results taking into account the orbital polarization (OP) correction[19]. The noncollinear calculations presented here were performed including the spin-orbit coupling. Hence, all calculated magnetic properties are influenced by exchange and relativistic effects, on equal footing, by the relativistic Kohn-Sham equation. This means that implicitly Heisenberg exchange, Dzyaloshinskii-Morya (DM) and magnetic anisotropy effects (MAE) are included in these calculations, albeit the DM and MAE interactions are not explicitly identified in the self-consistent calculations, whereas the exchange interaction in some cases is explicitly extracted from the calculations.

Here, we have considered Ni and Fe nanowires, and Ni-Pt and Fe-Pt alloy nanowires, with different sizes, supported on a Pt(111) surface. The Pt substrate was simulated by a cluster containing $\sim$ 5000 atoms located in a fcc lattice with the experimental lattice parameter of Pt. In order to provide a basis for the wave function in the vicinity of the surface and to treat charge transfers correctly, we included two overlayers of empty spheres (ES) above the Pt surface. The continued fraction that occurs in the recursion method was terminated with the Beer-Pettifor terminator[49] after 20 recursion levels. The calculations of the Ni and Fe nanostructures were performed by embedding the clusters as a perturbation on the self-consistently converged Pt(111) surface. The Fe and Ni sites and those of the closest shell of Pt (or empty spheres) sites around the defect were recalculated self-consistently, with sizes varying from 9 up to 69 sites, while the electronic structure for all other sites were kept

unchanged at their clean surface values. Lattice relaxations were neglected in most of the systems considered in this study. Some examples including structural relaxation are also presented, showing how the calculation without relaxation should give a reliable theoretical description of the magnetic behavior of the studied nanoclusters on Pt(111) substrate.

1. Khajetoorians, A. A., Wiebe, J., Chilian, B. & Wiesendanger, R. Realizing all-spin-based logic operations atom by atom. *Science* **332**, 1062–1064 (2011).
2. Serrate, D. *et al.* Imaging and manipulating the spin direction of individual atoms. *Nature Nanotechnology* **5**, 350–352 (2010).
3. Lounis, S., Dederichs, P. H. & Blügel, S. Magnetism of nanowires driven by novel even-odd effects. *Phys. Rev. Lett.* **101**, 107204 (2008).
4. Bergman, A., Nordström, L., Klautau, A. B., Frota-Pessôa, S. & Eriksson, O. Magnetic structures of small Fe, Mn, and Cr clusters supported on Cu(111): Noncollinear first-principles calculations. *Phys. Rev. B* **73**, 174434 (2006).
5. Igarashi, R. N., Klautau, A. B., Muniz, R. B., Sanyal, B. & Petrilli, H. M. First-principles studies of complex magnetism in Mn nanostructures on the Fe(001) surface. *Phys. Rev B* **85**, 014436 (2012).
6. Wahl, P. *et al.* Exchange interaction between single magnetic atoms. *Phys. Rev. Lett.* **98**, 056601 (2007).
7. Balashov, T. *et al.* Magnetic anisotropy & magnetization dynamics of individual atoms and clusters of Fe and Co on Pt(111). *Phys. Rev. Lett.* **102**, 257203 (2009).
8. Meier, F., Zhou, L., Wiebe, J. & Wiesendanger, R. Revealing magnetic interactions from single-atom magnetization curves. *Science* **320**, 82–86 (2008).
9. Zhou, L. *et al.* Strength and directionality of surface Ruderman-Kittel-Kasuya-Yosida interaction mapped on the atomic scale. *Nature Physics* **6**, 187–191 (2010).
10. Gambardella, P. *et al.* Giant magnetic anisotropy of single cobalt atoms and nanoparticles. *Science* **300**, 1130–1133 (2003).
11. Dallmeyer, A. *et al.* Electronic states and magnetism of monatomic Co and Cu wires. *Phys. Rev B* **61**, R5133 (2000).
12. Gambardella, P. & Kern, K. Ni growth on vicinal Pt(1 1 1): low temperature exchange and formation of ordered surface alloys. *Surf. Sci.* **475**, L229 (2001).
13. Honolka, J. *et al.* Magnetism of FePt Surface Alloys. *Phys. Rev. Lett.* **102**, 067207 (2009).
14. Honolka, J. *et al.* Complex magnetic phase in submonolayer Fe stripes on Pt(997). *Phys. Rev. B* **79**, 104430 (2009).
15. Hirjibehedin, C. F., Lutz, C. P. & Heinrich, A. J. Spin Coupling in Engineered Atomic Structures. *Science* **312**, 1021–1024 (2006).
16. Khajetoorians, A. A. *et al.* Atom-by-atom engineering and magnetometry of tailored nanomagnets. *Nature Phys.* **8**, 497–503 (2012).
17. Brovko, O. O., Ignatiev, P. A., Stepanyuk, V. S. & Bruno, P. Tailoring exchange interactions in engineered nanostructures: An *ab initio* study. *Phys. Rev. Lett.* **101**, 036809 (2008).
18. Essolaani, W. *et al.* Formation of one-dimensional ordered alloy at step edges: An atomistic study of the (2×1) Ni/Pt alloy on the Pt(997) surface. *Surf. Sci.* **605**, 917 (2011).
19. Eriksson, O., Johansson, B., Albers, R. C., Boring, A. M. & Brooks, M. S. S. Orbital magnetism in Fe, Co, and Ni. *Phys. Rev. B* **42**, 2707 (1990).
20. Frota-Pessôa, S. Magnetic behavior of 3d impurities in Cu, Ag, and Au: First-principles calculations of orbital moments. *Phys. Rev. B* **69**, 104401 (2004).
21. Brewer, W. D. *et al.* Direct observation of orbital magnetism in cubic solids. *Phys. Rev. Lett.* **93**, 077205 (2004).
22. Stearns, M. B. *3d, 4d and 5d Elements, Alloys and Compounds*, Volume **19** (Springer-Verlag, Berlin, 1986).
23. Frota-Pessôa, S., Klautau, A. B. & Legoas, S. B. Influence of interface mixing on the magnetic properties of Ni/Pt multilayers. *Phys. Rev. B* **66**, 132416 (2002).
24. Wilhelm, F. *et al.* Layer-resolved magnetic moments in Ni/Pt multilayers. *Phys. Rev. Lett.* **85**, 413 (2000).
25. Poulopoulos, P. *et al.* X-ray magnetic circular dichroic magnetometry on Ni/Pt multilayers. *J. Appl. Phys.* **89**, 3874 (2001).
26. Wilhelm, F. *et al.* Magnetic anisotropy energy and the anisotropy of the orbital moment of Ni in Ni/Pt multilayers. *Phys. Rev. B* **61**, 8647 (2000).
27. Bornemann, S. *et al.* Trends in the magnetic properties of Fe, Co, and Ni clusters and monolayers on Ir(111), Pt(111), and Au(111). *Phys. Rev. B* **86**, 104436 (2012).
28. Ruderman, M. A. & Kittel, C. Indirect exchange coupling of nuclear magnetic moments by conduction electrons. *Phys. Rev.* **96**, 99 (1954).
29. Mohn, P. *Magnetism in the Solid State. An Introduction* (Springer-Verlag, 2003).
30. Patrone, P. N. & Einstein, T. L. Anisotropic surface-state-mediated RKKY interaction between adatoms. *Phys. Rev.* **85**, 045429 (2012).
31. Wiebe, J. *et al.* Unoccupied surface state on Pt(111) revealed by scanning tunneling spectroscopy. *Phys. Rev. B* **72**, 193406 (2005).
32. Frota-Pessôa, S., Muniz, R. B. & Kudrnovský, J. Exchange coupling in transition-metal ferromagnets. *Phys. Rev. B* **62**, 5293 (2000).
33. Liechtenstein, A. I., Katsnelson, M. I., Antropov, V. P. & Gubanov, V. A. Local spin density functional approach to the theory of exchange interactions in ferromagnetic metals and alloys. *J. Magn. Magn. Mater.* **67**, 65 (1987).
34. Oka, H. *et al.* Spin-dependent quantum interference within a single magnetic nanostructure. *Science* **327**, 843–846 (2010).
35. Rusponi, S. *et al.* The remarkable difference between surface and step atoms in the magnetic anisotropy of two-dimensional nanostructures. *Nature Mat.* **2**, 546–551 (2003).
36. Lounis, S. & Dederichs, P. Mapping the magnetic exchange interactions from first principles: Anisotropy anomaly and application to Fe, Ni, and Co. *Phys. Rev. B* **82**, 180404(R) (2010).
37. Cracknell, A. P. Time-Reversal Degeneracies in the Band. Structure of a Ferromagnetic Metal. *Phys. Rev. B* **1**, 1261 (1970).
38. Singh, M., Callaway, J. & Wang, C. S. Calculation of g and g′ for iron and nickel. *Phys. Rev. B* **14**, 1214 (1976).
39. Brooks, M. S. S. & Kelly, P. J. Large Orbital-Moment Contribution to 5f Band Magnetism. *Phys. Rev. Lett.* **51**, 1708 (1983).
40. Mankovsky, S. *et al.* Effects of spin-orbit coupling on the spin structure of deposited transition-metal clusters. *Phys. Rev. B* **80**, 014422 (2009).
41. Etz, C., Costa, M., Eriksson, O. & Bergman, A. Accelerating the switching of magnetic nanoclusters by anisotropy-driven magnetization dynamics. *Phys. Rev. B* **86**, 224401 (2012).
42. Peduto, P. R., Frota-Pessôa, S. & Methfessel, M. S. First-principles linear muffin-tin orbital atomic-sphere approximation calculations in real space. *Phys. Rev. B* **44**, 13283 (1991).
43. Frota-Pessôa, S. First-principles real-space linear-muffin-tin-orbital calculations of 3d impurities in Cu. *Phys. Rev. B* **46**, 14570 (1992).
44. Bergman, A., Nordström, L., Klautau, A. B., Frota-Pessôa, S. & Eriksson, O. Magnetic structures of small Fe, Mn, and Cr clusters supported on Cu(111): Noncollinear first-principles calculations. *Phys. Rev. B* **75**, 224425 (2007).
45. Bergman, A., Nordström, L., Klautau, A. B., Frota-Pessôa, S. & Eriksson, O. Non-collinear magnetization of V clusters supported on a Cu (1 1 1) surface: Theory. *Surf. Sci.* **600**, 4838 (2006).
46. Andersen, O. K., Jepsen, O. & Glötzel, D. *Highlights of Condensed-Matter Theory* (North Holland, 1985).
47. Haydock, R. *Solid State Physics*, Volume **35**, (Academic Press, New York, 1980).
48. von Barth, U. & Hedin, L. A. A local exchange-correlation potential for the spin polarized case. *J. Phys. C.* **5**, 1629 (1972).
49. Beer, N. & Pettifor, D. *The Electronic Structure of Complex Systems* (Plenum Press, New York, 1984).
50. Kasuya, T. A Theory of metallic ferro- and antiferromagnetism on Zenerś model. *Progr. Theor. Phys.* **16**, 45 (1956).
51. Yosida, K. Magnetic properties of Cu-Mn alloys. *Phys. Rev.* **106**, 893 (1957).

Acknowledgements

We acknowledge financial support from the Swedish Research Council, the Swedish Foundation for Strategic Research, CAPES, FAPESPA, VALE, and CNPq, Brazil. The calculations were performed at the computational facilities of the CENAPAD at University of Campinas, SP, Brazil. O. E. acknowledges the Swedish research Council, the KAW foundation and the ERC (project 247062 - ASD). O. E. and A. B. are, in addition, grateful for support from eSSENCE.

Author contributions

M.M.B.-N. and M.S.R. carried out the numerical calculations. B.S., A.B., R.B.M., O.E. and A.B.K. discussed the results and prepared the manuscript.

Additional information

Competing financial interests: The authors declare no competing financial interests.

How to cite this article: Bezerra-Neto, M.M. *et al.* Complex magnetic structure of clusters and chains of Ni and Fe on Pt(111). *Sci. Rep.* **3**, 3054; DOI:10.1038/srep03054 (2013).